Arterial Traffic Signal Coordination for General and Public Transport Vehicles Using Dedicated Lanes

Krzysztof Florek, Ph.D.[1]

Abstract: Coordination of traffic signals is one of the most effective methods to improve the quality of traffic control on an artery. Properly coordinated traffic signals can effectively minimize delay and number of stops, increase travel speed, and reduce the number of collisions. MULTIBAND and AM-BAND are well known and widely used methods for arterial traffic control. The optimum solution provides the ability to travel without stops for most individual vehicles, whereas buses stopping at bus stops may experience excessive delays. This paper presents BUS-MULTIBAND and BUS-AM-BAND methods formulated as mixed-integer linear programs that solve the signal coordination problem for passenger cars and public transport vehicles simultaneously. The optimal signal coordination plans for general and transit vehicles were computed, simulated, and compared with signal plans generated for only general vehicles. Simulation results indicate that traffic signal coordination plans generated by the proposed methods can provide significant benefits for buses and, at most, small losses for general vehicles compared with plans generated by MULTIBAND and AM-BAND. **DOI: 10.1061/JTEPBS.0000374.**

Author keywords: Traffic signal coordination; MULTIBAND; AM-BAND; Mixed-integer linear programming; Traffic simulation.

Introduction

Growing congestion, particularly in the centers of large cities, increases travel time, traffic emissions, and the number of collisions; therefore, the authorities of most modern cities are trying to construct communication systems on the basis of the principle of sustainable development, with an emphasis on the development of public transport. The aim is to improve the standard of service provided by public transport, which should increase the popularity of this mode of transport and reduce congestion on most crowded streets. One of the most effective solutions to favor public transport is bus lanes that allow buses smooth movement along the most crowded streets. The potential benefits from the implementation of such solutions is primarily an improvement in communication speed, punctuality, and attractiveness of public transport. Coordination of traffic lights, however, usually is designed for general vehicles, which with appropriate offsets can travel along the entire arterial without stopping. The progression band is the part of the cycle time that allows most vehicles to traverse the arterial without stopping. By maximizing the width of green bands in both directions along an artery, vehicular progression through successive traffic lights can be maintained and the total delay and number of stops can be minimized. Public transport vehicles that stop at a bus stop leave the progression band and are forced to stop at the next intersection, unlike general vehicles that travel in the progression band. Traffic signal coordination calculated only for general vehicles generates considerable unwanted delays and a large number of stops for buses on streets with bus lanes.

In this paper, an improvement to the public transport version of bandwidth-based arterial traffic signal coordination models, MULTIBAND (Gartner et al. 1991) and AM-BAND (Zhang et al. 2015), were developed and tested. The formulation is based on mixed-integer linear programming and is solved by Octave 4.2. This new version concurrently calculates two independent progression bands: one for general vehicles, and the other for buses on bus lanes stopping at bus stops localized between adjacent intersections. Vehicles and buses travel along an artery on separate lanes with different speeds, but both progression bands are linked by common cycles and offsets. Compared with MULTIBAND and AM-BAND, the proposed model provides significant benefits for buses and, at most, minor losses for general vehicles.

Literature Review

Bandwidth maximization methods play an important role in traffic control practice, and their continuous improvement is of interest to many traffic engineers. Given the abundance of the literature in this area, it is impossible to provide an exhaustive review. Morgan and Little (1964) first presented a model to maximize the two-way progression bandwidth on an arterial. Little (1966) further proposed a model to concurrently optimize the common cycle length, progression speeds, and offsets with mixed-integer linear programming. An enhanced version of this model, MAXBAND (Little et al. 1981), was developed to account for left-turn treatments and the impact of initial queues. A main limitation of MAXBAND is that it does not take into account the actual traffic volume and flow capacity of each link, but uses only the average ratio of inbound and outbound traffic volumes in the signal optimization model. On the basis of MAXBAND, an optimization model with variable bandwidth was formulated (Gartner et al. 1991), MULTIBAND, to reflect the need for different bandwidths for links with different volumes. MULTIBAND introduces several significant extensions based on MAXBAND, including left-turn phase sequence optimization, initial queue clearance time, and variable bandwidths corresponding to each link's traffic characteristics. Although MULTIBAND relaxes the same band constraints, a part of the available band still cannot be utilized; therefore, an asymmetrical and multiband model,

[1]Dept. of Transportation Systems, Faculty of Civil Engineering, Cracow Univ. of Technology, 24 Warszawska St., Krakow 31-155, Poland. ORCID: https://orcid.org/0000-0001-7370-8884. Email: kflorek@pk.edu.pl

Note. This manuscript was submitted on February 28, 2019; approved on January 13, 2020; published online on April 24, 2020. Discussion period open until September 24, 2020; separate discussions must be submitted for individual papers. This paper is part of the ***Journal of Transportation Engineering, Part A: Systems***, © ASCE, ISSN 2473-2907.

AM-BAND, was proposed (Zhang et al. 2015) which relaxes the symmetrical constraints in MULTIBAND. This model increases bandwidth and thus reduces the number of stops and the delay time of vehicles. The artery coordination problem then was extended to grid networks. Chang et al. (1988) implemented the MAXBAND model in a multiarterial network and developed the MAXBAND-86 model. Chaudhary and Messer (1993) developed an arterial traffic signal coordination program called PASSER-IV, which is designed to optimize traffic signal timings for arterials and multiarterial closed-loop networks based on the MAXBAND model. Similarly, a network version of MULTIBAND named MULTIBAND-96 was developed (Stamatiadis and Gartner 1996). However, such extensions may significantly increase the computational complexity due to the expanded size of an integer variable set. To overcome this problem, a restricted branch and bound approach (Pillai et al. 1998), a two-step solution procedure (Gartner and Stamatiadis 2002), and a problem partition technique (Tian and Urbanik 2007; Zhang et al. 2016) were proposed which can improve the computational efficiency of existing progression models.

In recent years, other studies have been conducted on arterial traffic signal coordination. Lu et al. (2008) incorporated a traffic flow dispersion module in MAXBAND to address a limitation of the MAXBAND model which assumes that all vehicles travel at the same speed. Tian et al. (2008) conducted quantitative evaluations of two signal-timing issues (phase sequence and number of intersections) related to the progression bandwidth. Most studies have been devoted to the maximization of the progression band for through-traffic flows over the arterial which is assumed to have the highest volume among all traffic movements. Yang et al. (2015) proposed a multipath progression model which can maximize the progression band for all path flows with significant volume. Zhou et al. (2017) proposed an uneven double-cycle control method for arteries with some minor intersections whose actual signal cycle length is approximately half the common signal cycle length.

MAXBAND, MULTIBAND, and AM-BAND are designed for solving arterial signal coordination for general vehicles, but they are not entirely suitable for public transit because there is no time for stopping at stations in the bandwidth. Jeong and Kim (2014) modeled TRAMBAND by considering stops at stations, in which a fixed and narrow band for one tram is proposed, whereas the progression band for general vehicles is maximized. A fixed narrow band for trams requires a fixed dwell time, which can be achieved by adding additional waiting time at each station which can absorb dwell-time variability. Stops and delay at intersections for trams decreased in TRAMBAND compared with MAXBAND, whereas general vehicle delay increased slightly. Similarly, Dai et al. (2016) introduced a progression model for bus green bands. To establish the bus progression band, the main street is divided into parts based on the locations of the bus stops, then mixed-integer linear programming is employed to optimize the bandwidth for each group of intersections and connect the green bands for adjacent groups. Zhou et al. (2016) introduced a progression model only for trams based on modified AM-BAND by incorporating trams' dwell time at stations and minimum bandwidth value constraints to consider long tram body length. Ma et al. (2019) proposed a multimodal signal-coordination model, PM-BAND, which permits the progression bands' partition if necessary. For transit vehicles, the progression bands have fixed bandwidth for one vehicle, whereas for passenger cars it is maximized. The model optimizes signal coordination, system partition, and waiting time of transit vehicles. The travel time along the arteries is much more uncertain for buses than for cars due to the variability of the stopping time at the stations. To overcome this problem, a bus progression model which directly takes into account dwell time variability and capacity of bus stops was proposed (Kim et al. 2019).

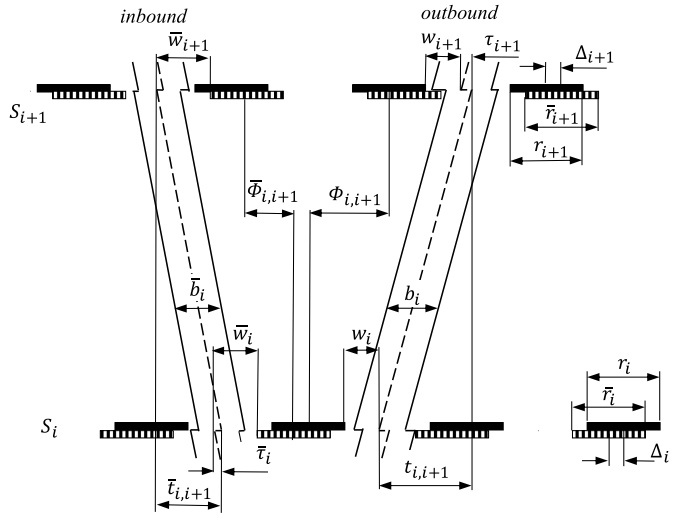

Fig. 1. Time-space diagram for MULTIBAND.

Most of the aforementioned signal coordination methods for public transit were developed on the basis of MAXBAND, and usually they assume a fixed progression band for public transport and try to maximize the band for general vehicles, or they focus on the progression band for public transport only. This study extended the MULTIBAND and AM-BAND models with bandwidth optimization for public transport vehicles stopping at stations and using dedicated lanes. In the next section, MULTIBAND and AM-BAND models are briefly presented, and then the extended models are described in detail.

Methodology

Basic progression models MULTIBAND and AM-BAND, and the proposed extended models, are modeled on a two-way arterial with n intersections. All intersections are controlled by a fixed-time strategy. The two travel directions along the artery are referred to as inbound and outbound, respectively.

MULTIBAND

MULTIBAND is an arterial signal coordination model formulated as a mixed-integer linear program. There are green bands for two travel directions along the arterial, called outbound and inbound. The traffic signal at each intersection i is denoted S_i (Fig. 1). Assuming that intersections are numbered sequentially from 1 to n in the outbound direction, the MULTIBAND model is defined in Eqs. (1)–(10). The decision variables include b_i, $\bar{b}_i$, z, w_i, $\bar{w}_i$, t_i, $\bar{t}_i$, δ_i, $\bar{\delta}_i$, and m_i

$$\max B = \frac{1}{n-1}\sum_{i=1}^{n-1}(a_i b_i + \bar{a}_i \bar{b}_i) \tag{1}$$

$$(1-k_i)\bar{b}_i \geq (1-k_i)k_i b_i \quad i = 1, \ldots, n-1 \tag{2}$$

$$\frac{1}{C_2} \leq z \leq \frac{1}{C_1} \tag{3}$$

$$\begin{aligned}
&\frac{1}{2}b_i \le w_i \le (1-r_i) - \frac{1}{2}b_i \\
&\frac{1}{2}b_i \le w_{i+1} + \tau_{i+1} \le (1-r_{i+1}) - \frac{1}{2}b_i \\
&\frac{1}{2}\bar{b}_i \le \bar{w}_i - \bar{\tau}_i \le (1-\bar{r}_i) - \frac{1}{2}\bar{b}_i \\
&\frac{1}{2}\bar{b}_i \le \bar{w}_{i+1} \le (1-\bar{r}_{i+1}) - \frac{1}{2}\bar{b}_i
\end{aligned} \quad i = 1, \ldots, n-1 \tag{4}$$

$$\begin{aligned}
&(w_i + \bar{w}_i) - (w_{i+1} + \bar{w}_{i+1}) + (t_i + \bar{t}_i) + \delta_i L_i - \bar{\delta}_i \bar{L}_i \\
&\quad - \delta_{i+1} L_{i+1} + \bar{\delta}_{i+1} \bar{L}_{i+1} - m_i = (r_{i+1} - r_i) + (\tau_{i+1} + \bar{\tau}_i) \\
&\quad i = 1, \ldots, n-1
\end{aligned} \tag{5}$$

$$\begin{aligned}
&\frac{d_i}{f_i} z \le t_i \le \frac{d_i}{e_i} z \\
&\frac{\bar{d}_i}{\bar{f}_i} z \le \bar{t}_i \le \frac{\bar{d}_i}{\bar{e}_i} z
\end{aligned} \quad i = 1, \ldots, n-1 \tag{6}$$

$$\begin{aligned}
&\frac{d_i}{h_i} z \le \frac{d_i}{d_{i+1}} t_{i+1} - t_i \le \frac{d_i}{g_i} z \\
&\frac{\bar{d}_i}{\bar{h}_i} z \le \frac{\bar{d}_i}{\bar{d}_{i+1}} \bar{t}_{i+1} - \bar{t}_i \le \frac{\bar{d}_i}{\bar{g}_i} z
\end{aligned} \quad i = 1, \ldots, n-2 \tag{7}$$

$$b_i, \bar{b}_i, w_i, \bar{w}_i \ge 0 \tag{8}$$

$$m_i = \text{ integer} \tag{9}$$

$$\delta_i, \bar{\delta}_i = \text{binary} \tag{10}$$

The objective function of MULTIBAND [Eq. (1)] is to maximize the weighted sum of bandwidths of the outbound and inbound directions. The bandwidths are weighted based on their corresponding road segments' volume to saturation flow rate ratios. Constraint Eq. (2) allows the arterial direction with a higher traffic volume to have a wider progression band. Constraint Eq. (3) defines the lower and upper limits of cycle length; the reciprocals are used here so that the remaining constraints can be expressed in linear form. Constraint Eq. (4) is an interference constraint which ensures that the left and right boundaries do not interfere with the corresponding edges of red signals. Constraint Eq. (5) is the well-known loop integer constraint, which states that the sum of internode and intranode offsets is an integer variable. It establishes the relationship among signal timing, bandwidth, travelling speed, and left-turn phase sequence. Constraint Eq. (6) imposes upper and lower limits on the travel speed of each segment, and Eq. (7) is the speed change between consecutive segments. Other constraints limit decision variables to non-negative Eq. (8) or integer/binary Eqs. (9) and (10) values.

AM-BAND

The AM-BAND model was developed by relaxing the symmetrical progression band requirement in MULTIBAND. In this model, the progression band for each directional road section (both outbound and inbound) is separated into two components (Fig. 2), represented by b_i^1 and b_i^2 for outbound and $\bar{b}_i^1$ and $\bar{b}_i^2$ for inbound, which do not need to be equal, i.e., the progression bands do not need to be symmetrical along the progression line. The decision variables include b_i^1, b_i^2, $\bar{b}_i^1$, $\bar{b}_i^2$, z, w_i, $\bar{w}_i$, t_i, $\bar{t}_i$, δ_i, $\bar{\delta}_i$, and m_i

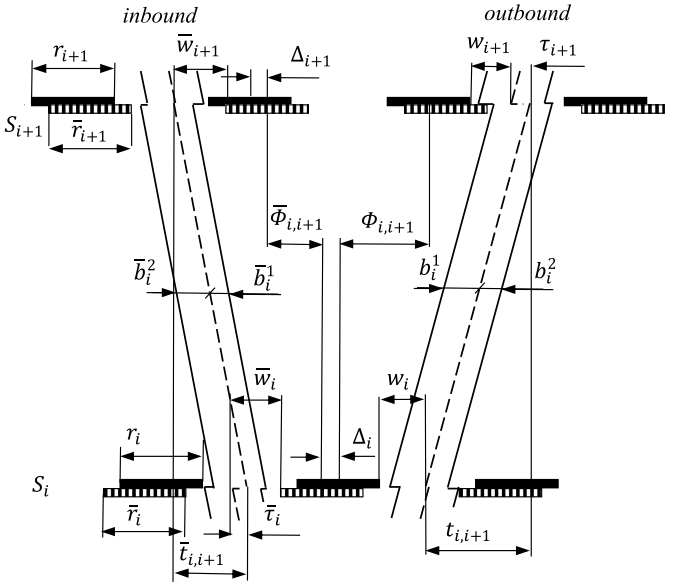

Fig. 2. Time-space diagram for AM-BAND.

$$\max B = \frac{1}{n-1} \sum_{i=1}^{n-1} [a_i (b_i^1 + b_i^2) + \bar{a}_i (\bar{b}_i^1 + \bar{b}_i^2)] \tag{11}$$

$$(1-k_i)(\bar{b}_i^1 + \bar{b}_i^2) \ge (1-k_i) k_i (b_i^1 + b_i^2) \quad i = 1, \ldots, n-1 \tag{12}$$

$$\frac{1}{C_2} \le z \le \frac{1}{C_1} \tag{13}$$

$$\begin{aligned}
&b_i^1 \le w_i \le (1-r_i) - b_i^2 \\
&b_i^1 \le w_{i+1} + \tau_{i+1} \le (1-r_{i+1}) - b_i^2 \\
&\bar{b}_i^1 \le \bar{w}_i - \bar{\tau}_i \le (1-\bar{r}_i) - \bar{b}_i^2 \\
&\bar{b}_i^1 \le \bar{w}_{i+1} \le (1-\bar{r}_{i+1}) - \bar{b}_i^2
\end{aligned} \quad i = 1, \ldots, n-1 \tag{14}$$

$$\begin{aligned}
&\frac{1}{q} b_i^2 \le b_i^1 \le q b_i^2 \\
&\frac{1}{q} \bar{b}_i^2 \le \bar{b}_i^1 \le q \bar{b}_i^2
\end{aligned} \quad i = 1, \ldots, n-1 \tag{15}$$

$$\begin{aligned}
&(w_i + \bar{w}_i) - (w_{i+1} + \bar{w}_{i+1}) + (t_i + \bar{t}_i) + \delta_i L_i - \bar{\delta}_i \bar{L}_i \\
&\quad - \delta_{i+1} L_{i+1} + \bar{\delta}_{i+1} \bar{L}_{i+1} - m_i = (r_{i+1} - r_i) + (\tau_{i+1} + \bar{\tau}_i) \\
&\quad i = 1, \ldots, n-1
\end{aligned} \tag{16}$$

$$\begin{aligned}
&\frac{d_i}{f_i} z \le t_i \le \frac{d_i}{e_i} z \\
&\frac{\bar{d}_i}{\bar{f}_i} z \le \bar{t}_i \le \frac{\bar{d}_i}{\bar{e}_i} z
\end{aligned} \quad i = 1, \ldots, n-1 \tag{17}$$

$$\begin{aligned}
&\frac{d_i}{h_i} z \le \frac{d_i}{d_{i+1}} t_{i+1} - t_i \le \frac{d_i}{g_i} z \\
&\frac{\bar{d}_i}{\bar{h}_i} z \le \frac{\bar{d}_i}{\bar{d}_{i+1}} \bar{t}_{i+1} - \bar{t}_i \le \frac{\bar{d}_i}{\bar{g}_i} z
\end{aligned} \quad i = 1, \ldots, n-2 \tag{18}$$

$$b_i^1, b_i^2, \bar{b}_i^1, \bar{b}_i^2, w_i, \bar{w}_i \ge 0 \tag{19}$$

$$m_i = \text{ integer} \tag{20}$$

$$\delta_i, \bar{\delta}_i = \text{binary} \tag{21}$$

In the objective function Eq. (11) and directional preference constraints Eq. (12), bands b_i and $\bar{b}_i$ are replaced by the sum of left and right bands $b_i^1 + b_i^2$ and $\bar{b}_i^1 + \bar{b}_i^2$, respectively. Corresponding changes are made to the interference constraints Eq. (13), in which, instead of half of a green band, the left and right bands are inserted. Constraint Eq. (14) defines the degree of band asymmetry, where $q = 2$ is suggested (Zhang et al. 2015). This constraint ensures that the left or right part of a progression band is nonzero. The rest of constraints Eqs. (16)–(21) are the same as in the MULTIBAND model.

BUS-MULTIBAND with Dedicated Bus Lanes

When there are dedicated bus lanes, coordination problems for general vehicles and buses are to a great extent independent. Both classes of vehicles share common traffic control at consecutive intersections, but they can travel along the artery at different speeds, and buses have to stop at bus stops; therefore, most of the constraints of the MULTIBAND model are replicated for buses. Fig. 3 presents a time-space diagram of green bands for general vehicles and buses.

The objective function is complemented by the weighted sum of green bands for buses

$$\max B = \frac{1}{n-1}\sum_{i=1}^{n-1}(a_i b_i + \bar{a}_i \bar{b}_i + a_i^b b_i^b + \bar{a}_i^b \bar{b}_i^b) \tag{22}$$

The weighting coefficients for general vehicles are calculated as a volume-to-saturation flow rate ratio. Saturation flow rate for buses generally is irrelevant, but for compatibility with the original MULTIBAND model, weighting coefficients are calculated in a similar way as for general vehicles

$$a_i^b = \left(\frac{V_i^b}{S_i^b}\right)^p$$
$$\bar{a}_i^b = \left(\frac{\bar{V}_i^b}{\bar{S}_i^b}\right)^p \tag{23}$$

Weighting coefficients Eq. (23) calculated similarly for buses and cars as a volume-to-saturation flow ratio will favor individual vehicles, and the progression band for buses should not substantially worsen the progression band for cars. On the other hand, buses carry many more passengers, and different weighting coefficients such as load or occupancy may be considered.

Directional preference for buses can be expressed as for general vehicles, but bus volumes in both directions usually are the same, so $k_i^b = 1$

$$(1 - k_i^b)\bar{b}_i^b \geq (1 - k_i^b) k_i^b b_i^b \tag{24}$$

Alternatively, Eq. (25) can be used, but a strict equality can restrict one band to a specific value once the other band has reached its maximum potential

$$\bar{b}_i^b = b_i^b \tag{25}$$

Interference constraints for buses are

$$\frac{1}{2} b_i \leq w_i \leq (1 - r_i) - \frac{1}{2} b_i$$
$$\frac{1}{2} b_i \leq w_{i+1} + \tau_{i+1} \leq (1 - r_{i+1}) - \frac{1}{2} b_i$$
$$\frac{1}{2} \bar{b}_i \leq \bar{w}_i - \bar{\tau}_i \leq (1 - \bar{r}_i) - \frac{1}{2} \bar{b}_i$$
$$\frac{1}{2} \bar{b}_i \leq \bar{w}_{i+1} \leq (1 - \bar{r}_{i+1}) - \frac{1}{2} \bar{b}_i \tag{26}$$

Loop integer constraint for buses are

$$\Phi_{i,i+1}^b + \bar{\Phi}_{i,i+1}^b + \Delta_i - \Delta_{i+1} = m_i^b \tag{27}$$

Substituting $\Phi_{i,i+1}^b$, $\bar{\Phi}_{i,i+1}^b$, Δ_i, and Δ_{i+1} calculated as for general vehicles gives

$$(w_i^b + \bar{w}_i^b) - (w_{i+1}^b + \bar{w}_{i+1}^b) + (t_i^b + \bar{t}_i^b) + \delta_i L_i - \bar{\delta}_i \bar{L}_i - \delta_{i+1} L_{i+1} + \bar{\delta}_{i+1} \bar{L}_{i+1} - m_i^b = (r_{i+1} - r_i) + (\tau_{i+1}^b + \bar{\tau}_i^b) \tag{28}$$

Coordination problems for general vehicles and buses are connected by the constraint that internode offsets for both classes of vehicles can differ by an integer number of cycles

$$\Phi_{i,i+1}^b - \Phi_{i,i+1} = m_i^{gb} \tag{29}$$

where

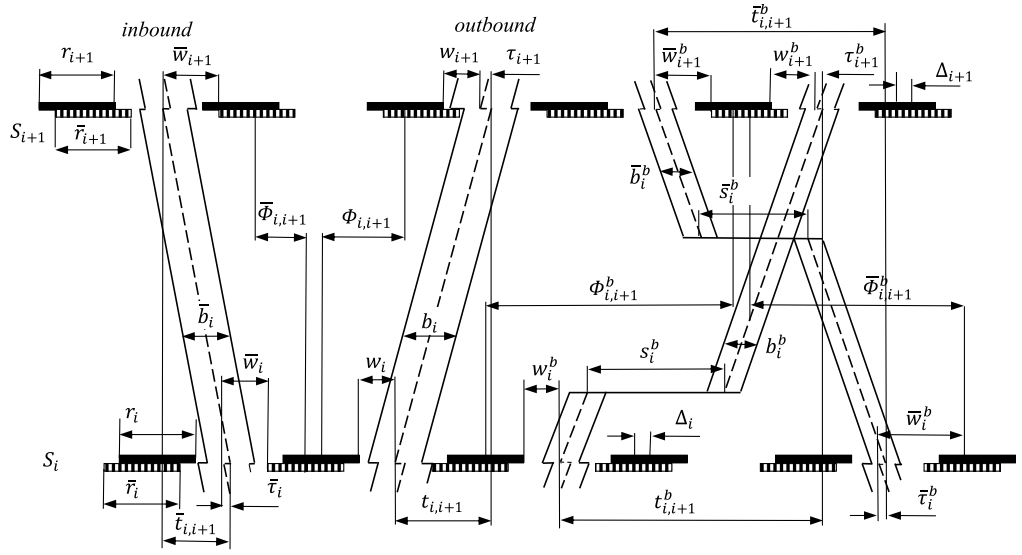

Fig. 3. Time-space diagram for BUS-MULTIBAND.

J. Transp. Eng., Part A: Systems, 2020, 146(7): 04020051

$$\Phi_{i,i+1} + \frac{1}{2} r_{i+1} + w_{i+1} + \tau_{i+1} = \frac{1}{2} r_i + w_i + t_{i,i+1} \tag{30}$$

$$\Phi^b_{i,i+1} + \frac{1}{2} r_{i+1} + w^b_{i+1} + \tau^b_{i+1} = \frac{1}{2} r_i + w^b_{i+1} + t^b_{i,i+1} \tag{31}$$

Substituting Eq. (30) and (31) into Eq. (29) gives

$$(w^b_i - w^b_{i+1}) - (w_i - w_{i+1}) + (t^b_{i,i+1} - t_{i,i+1}) - m^{gb}_i = (\tau^b_{i+1} - \tau_{i+1}) \tag{32}$$

Travel time for public transport vehicles include stop time at a bus stop (if it exists between intersections i and $i+1$), and hence constraints determining travel speed are modified compared with the case of general vehicles

$$\begin{aligned} &\frac{d_i}{f^b_i} z \le t^b_i - \varepsilon^b_i s^b_i \le \frac{d_i}{e^b_i} z \\ &\frac{\bar{d}_i}{\bar{f}^b_i} z \le \bar{t}^b_i - \bar{\varepsilon}^b_i \bar{s}^b_i \le \frac{\bar{d}_i}{\bar{e}^b_i} z \end{aligned} \tag{33}$$

where ε^b_i, ($\bar{\varepsilon}^b_i$) is a binary parameter, where 1 = bus stop in segment i outbound (inbound), and 0 = otherwise.

Speed change constraints for buses takes the form

$$\begin{aligned} &\frac{d_i}{h^b_i} z \le \frac{d_i}{d_{i+1}} (t^b_{i+1} - \varepsilon^b_{i+1} s^b_{i+1}) - (t^b_i - \varepsilon^b_i s^b_i) \le \frac{d_i}{g^b_i} z \\ &\frac{\bar{d}_i}{\bar{h}^b_i} z \le \frac{\bar{d}_i}{\bar{d}_{i+1}} (\bar{t}^b_{i+1} - \bar{\varepsilon}^b_{i+1} \bar{s}^b_{i+1}) - (\bar{t}^b_{i+1} - \bar{\varepsilon}^b_i \bar{s}^b_i) \le \frac{\bar{d}_i}{\bar{g}_i} z \end{aligned} \tag{34}$$

The optimization program determines the following decision variables: b_i, $\bar{b}_i$, b^b_i, $\bar{b}^b_i$, w_i, $\bar{w}_i$, w^b_i, $\bar{w}^b_i$, t_i, $\bar{t}_i$, t^b_i, $\bar{t}^b_i$, δ_i, $\bar{\delta}_i$, m_i, m^b_i, and m^{gb}_i

$$\max B = \frac{1}{n-1} \sum_{i=1}^{n-1} (a_i b_i + \bar{a}_i \bar{b}_i + a^b_i b^b_i + \bar{a}^b_i \bar{b}^b_i) \tag{35}$$

$$(1 - k_i) \bar{b}_i \ge (1 - k_i) k_i b_i \quad i = 1, \ldots, n-1 \tag{36}$$

$$(1 - k^b_i) \bar{b}^b_i \ge (1 - k^b_i) k^b_i b^b_i \quad i = 1, \ldots, n-1 \tag{37}$$

$$\frac{1}{C_{\max}} \le z \le \frac{1}{C_{\min}} \tag{38}$$

$$\begin{aligned} &\frac{1}{2} b_i \le w_i \le (1 - r_i) - \frac{1}{2} b_i \\ &\frac{1}{2} b_i \le w_{i+1} + \tau_{i+1} \le (1 - r_{i+1}) - \frac{1}{2} b_i \\ &\frac{1}{2} \bar{b}_i \le \bar{w}_i - \bar{\tau}_i \le (1 - \bar{r}_i) - \frac{1}{2} \bar{b}_i \\ &\frac{1}{2} \bar{b}_i \le \bar{w}_{i+1} \le (1 - \bar{r}_{i+1}) - \frac{1}{2} \bar{b}_i \end{aligned} \quad i = 1, \ldots, n-1 \tag{39}$$

$$\begin{aligned} &\frac{1}{2} b^b_i \le w^b_i \le (1 - r_i) - \frac{1}{2} b^b_i \\ &\frac{1}{2} b^b_i \le w^b_{i+1} + \tau^b_{i+1} \le (1 - r_{i+1}) - \frac{1}{2} b^b_i \\ &\frac{1}{2} \bar{b}^b_i \le \bar{w}^b_i - \bar{\tau}^b_i \le (1 - \bar{r}_i) - \frac{1}{2} \bar{b}^b_i \\ &\frac{1}{2} \bar{b}^b_i \le \bar{w}^b_{i+1} \le (1 - \bar{r}_{i+1}) - \frac{1}{2} \bar{b}^b_i \end{aligned} \quad i = 1, \ldots, n-1 \tag{40}$$

$$\begin{aligned} &(w_i + \bar{w}_i) - (w_{i+1} + \bar{w}_{i+1}) + (t_i + \bar{t}_i) + \delta_i L_i - \bar{\delta}_i \bar{L}_i - \delta_{i+1} L_{i+1} \\ &\quad + \bar{\delta}_{i+1} \bar{L}_{i+1} - m_i = (r_{i+1} - r_i) + (\tau_{i+1} + \bar{\tau}_i) \quad i = 1, \ldots, n-1 \end{aligned} \tag{41}$$

$$\begin{aligned} &(w^b_i + \bar{w}^b_i) - (w^b_{i+1} + \bar{w}^b_{i+1}) + (t^b_i + \bar{t}^b_i) + \delta_i L_i - \bar{\delta}_i \bar{L}_i - \delta_{i+1} L_{i+1} \\ &\quad + \bar{\delta}_{i+1} \bar{L}_{i+1} - m^b_i = (r_{i+1} - r_i) + (\tau^b_{i+1} + \bar{\tau}^b_i) \quad i = 1, \ldots, n-1 \end{aligned} \tag{42}$$

$$(w^b_i - w^b_{i+1}) - (w_i - w_{i+1}) + (t^b_{i,i+1} - t_{i,i+1}) - m^{gb}_i = (\tau^b_{i+1} - \tau_{i+1}) \quad i = 1, \ldots, n-1 \tag{43}$$

$$\begin{aligned} &\frac{d_i}{f_i} z \le t_i \le \frac{d_i}{e_i} z \\ &\frac{\bar{d}_i}{\bar{f}_i} z \le \bar{t}_i \le \frac{\bar{d}_i}{\bar{e}_i} z \end{aligned} \quad i = 1, \ldots, n-1 \tag{44}$$

$$\begin{aligned} &\frac{d_i}{f^b_i} z \le t^b_i - \varepsilon^b_i s^b_i \le \frac{d_i}{e^b_i} z \\ &\frac{\bar{d}_i}{\bar{f}^b_i} z \le \bar{t}^b_i - \bar{\varepsilon}^b_i \bar{s}^b_i \le \frac{\bar{d}_i}{\bar{e}^b_i} z \end{aligned} \quad i = 1, \ldots, n-1 \tag{45}$$

$$\begin{aligned} &\frac{d_i}{h_i} z \le \frac{d_i}{d_{i+1}} t_{i+1} - t_i \le \frac{d_i}{g_i} z \\ &\frac{\bar{d}_i}{\bar{h}_i} z \le \frac{\bar{d}_i}{\bar{d}_{i+1}} \bar{t}_{i+1} - \bar{t}_i \le \frac{\bar{d}_i}{\bar{g}_i} z \end{aligned} \quad i = 1, \ldots, n-1 \tag{46}$$

$$\begin{aligned} &\frac{d_i}{h^b_i} z \le \frac{d_i}{d_{i+1}} (t^b_{i+1} - \varepsilon^b_{i+1} s^b_{i+1}) - (t^b_i - \varepsilon^b_i s^b_i) \le \frac{d_i}{g^b_i} z \\ &\frac{\bar{d}_i}{\bar{h}^b_i} z \le \frac{\bar{d}_i}{\bar{d}_{i+1}} (\bar{t}^b_{i+1} - \bar{\varepsilon}^b_{i+1} \bar{s}^b_{i+1}) - (\bar{t}^b_{i+1} - \bar{\varepsilon}^b_i \bar{s}^b_i) \le \frac{\bar{d}_i}{\bar{g}_i} z \end{aligned} \quad i = 1, \ldots, n-1 \tag{47}$$

$$b_i, \bar{b}_i, b^b_i, \bar{b}^b_i, w_i, \bar{w}_i, w^b_i, \bar{w}^b_i \ge 0 \tag{48}$$

$$m_i, m^b_i, m^{gb}_i = \text{integer} \tag{49}$$

$$\delta_i, \bar{\delta}_i = \text{binary} \tag{50}$$

In the basic BUS-MULTIBAND model, the mean stop time, which is the dwell time for each station, is constant. Dwell times cannot be easily controlled because they depend on passenger volumes boarding and alighting at the stations. Stop time can be optimized assuming that the stop time is the sum of dwell time and additional waiting time

$$s^b_i = s^{bd}_i + s^{bw}_i \tag{51}$$

Waiting time extends the service time for the unloading and loading passengers and additionally can reduce stop time variability. Finally, stop time can be incorporated into the decision variable set with constraints

$$\begin{aligned} &s^b_{i\min} z \le s^b_i \le s^b_{i\max} z \\ &\bar{s}^b_{i\min} z \le \bar{s}^b_i \le \bar{s}^b_{i\max} z \end{aligned} \tag{52}$$

The optimization program BUS-MULTIBAND S determines the decision variables b_i, $\bar{b}_i$, b^b_i, $\bar{b}^b_i$, w_i, $\bar{w}_i$, w^b_i, $\bar{w}^b_i$, t_i, $\bar{t}_i$, t^b_i, $\bar{t}^b_i$, δ_i, $\bar{\delta}_i$, m_i, m^b_i, m^{gb}_i, s^b_i, and $\bar{s}^b_i$ with objective function Eq. (35) and constraints Eqs. (36)–(50) and (52).

BUS-AM-BAND with Dedicated Lanes

The extended model AM-BAND for general vehicles and buses is similar to the previous extension of MULTIBAND (Fig. 4).

The optimization program determines the following decision variables: b_i^1, b_i^2, $\bar{b}_i^1$, $\bar{b}_i^2$, b_i^{1b}, b_i^{2b}, $\bar{b}_i^1$, $\bar{b}_i^2$, w_i, $\bar{w}_i$, w_i^b, $\bar{w}_i^b$, t_i, $\bar{t}_i$, t_i^b, $\bar{t}_i^b$, δ_i, $\bar{\delta}_i$, m_i, m_i^b, and m_i^{gb}

$$\max B = \frac{1}{n-1}\sum_{i=1}^{n-1}[a_i(b_i^1 + b_i^2) + \bar{a}_i(\bar{b}_i^1 + \bar{b}_i^2) + a_i^b(b_i^{1b} + b_i^{2b}) + \bar{a}_i^b(\bar{b}_i^1 + \bar{b}_i^2)] \tag{53}$$

$$(1-k_i)(\bar{b}_i^1 + \bar{b}_i^2) \geq (1-k_i)k_i(b_i^1 + b_i^2) \quad i = 1, \ldots, n-1 \tag{54}$$

$$(1-k_i^b)(\bar{b}_i^{1b} + \bar{b}_i^{2b}) \geq (1-k_i^b)k_i^b(b_i^{1b} + b_i^{2b}) \quad i = 1, \ldots, n-1 \tag{55}$$

$$\frac{1}{C_2} \leq z \leq \frac{1}{C_1} \tag{56}$$

$$\begin{aligned} &b_i^1 \leq w_i \leq (1-r_i) - b_i^2 \\ &b_i^1 \leq w_{i+1} + \tau_{i+1} \leq (1-r_{i+1}) - b_i^2 \\ &\bar{b}_i^1 \leq \bar{w}_i - \bar{\tau}_i \leq (1-\bar{r}_i) - \bar{b}_i^2 \\ &\bar{b}_i^1 \leq \bar{w}_{i+1} \leq (1-\bar{r}_{i+1}) - \bar{b}_i^2 \end{aligned} \quad i = 1, \ldots, n-1 \tag{57}$$

$$\begin{aligned} &b_i^{1b} \leq w_i^b \leq (1-r_i) - b_i^{2b} \\ &b_i^{1b} \leq w_{i+1}^b + \tau_{i+1} \leq (1-r_{i+1}) - b_i^{2b} \\ &\bar{b}_i^{1b} \leq \bar{w}_i^b - \bar{\tau}_i \leq (1-\bar{r}_i) - \bar{b}_i^{2b} \\ &\bar{b}_i^{1b} \leq \bar{w}_{i+1}^b \leq (1-\bar{r}_{i+1}) - \bar{b}_i^{2b} \end{aligned} \quad i = 1, \ldots, n-1 \tag{58}$$

$$\begin{aligned} &\frac{1}{q}b_i^2 \leq b_i^1 \leq qb_i^2 \\ &\frac{1}{q}\bar{b}_i^2 \leq \bar{b}_i^1 \leq q\bar{b}_i^2 \end{aligned} \quad i = 1, \ldots, n-1 \tag{59}$$

$$\begin{aligned} &\frac{1}{q}b_i^{2b} \leq b_i^{1b} \leq qb_i^{2b} \\ &\frac{1}{q}\bar{b}_i^{2b} \leq \bar{b}_i^{1b} \leq q\bar{b}_i^{2b} \end{aligned} \quad i = 1, \ldots, n-1 \tag{60}$$

$$(w_i + \bar{w}_i) - (w_{i+1} + \bar{w}_{i+1}) + (t_i + \bar{t}_i) + \delta_i L_i - \bar{\delta}_i \bar{L}_i - \delta_{i+1}L_{i+1} + \bar{\delta}_{i+1}\bar{L}_{i+1} - m_i = (r_{i+1} - r_i) + (\tau_{i+1} + \bar{\tau}_i) \quad i = 1, \ldots, n-1 \tag{61}$$

$$(w_i^b + \bar{w}_i^b) - (w_{i+1}^b + \bar{w}_{i+1}^b) + (t_i^b + \bar{t}_i^b) + \delta_i L_i - \bar{\delta}_i \bar{L}_i - \delta_{i+1}L_{i+1} + \bar{\delta}_{i+1}\bar{L}_{i+1} - m_i^b = (r_{i+1} - r_i) + (\tau_{i+1}^b + \bar{\tau}_i^b) \quad i = 1, \ldots, n-1 \tag{62}$$

$$(w_i^b - w_{i+1}^b) - (w_i - w_{i+1}) + (t_{i,i+1}^b - t_{i,i+1}) - m_i^{gb} = (\tau_{i+1}^b - \tau_{i+1}) \quad i = 1, \ldots, n-1 \tag{63}$$

$$\frac{d_i}{f_i}z \leq t_i \leq \frac{d_i}{e_i}z \qquad \frac{\bar{d}_i}{\bar{f}_i}z \leq \bar{t}_i \leq \frac{\bar{d}_i}{\bar{e}_i}z \quad i = 1, \ldots, n-1 \tag{64}$$

$$\begin{aligned} &\frac{d_i}{f_i^b}z \leq t_i^b - \varepsilon_i^b s_i^b \leq \frac{d_i}{e_i^b}z \\ &\frac{\bar{d}_i}{\bar{f}_i^b}z \leq \bar{t}_i^b - \bar{\varepsilon}_i^b \bar{s}_i^b \leq \frac{\bar{d}_i}{\bar{e}_i^b}z \end{aligned} \quad i = 1, \ldots, n-1 \tag{65}$$

$$\begin{aligned} &\frac{d_i}{h_i}z \leq \frac{d_i}{d_{i+1}}t_{i+1} - t_i \leq \frac{d_i}{g_i}z \\ &\frac{\bar{d}_i}{\bar{h}_i}z \leq \frac{\bar{d}_i}{\bar{d}_{i+1}}\bar{t}_{i+1} - \bar{t}_i \leq \frac{\bar{d}_i}{\bar{g}_i}z \end{aligned} \quad i = 1, \ldots, n-1 \tag{66}$$

$$\begin{aligned} &\frac{d_i}{h_i^b}z \leq \frac{d_i}{d_{i+1}}(t_{i+1}^b - \varepsilon_{i+1}^b s_{i+1}^b) - (t_i^b - \varepsilon_i^b s_i^b) \leq \frac{d_i}{g_i^b}z \\ &\frac{\bar{d}_i}{\bar{h}_i^b}z \leq \frac{\bar{d}_i}{\bar{d}_{i+1}}(\bar{t}_{i+1}^b - \bar{\varepsilon}_{i+1}^b \bar{s}_{i+1}^b) - (\bar{t}_{i+1}^b - \bar{\varepsilon}_i^b \bar{s}_i^b) \leq \frac{\bar{d}_i}{\bar{g}_i}z \end{aligned} \quad i = 1, \ldots, n-1 \tag{67}$$

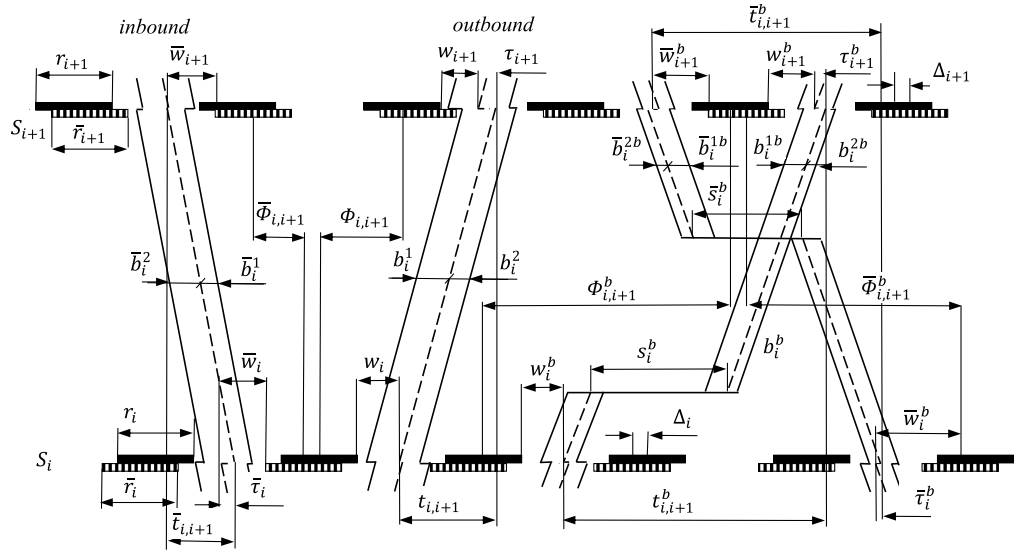

Fig. 4. Time-space diagram for BUS-AM-BAND.

$$b_i^1, b_i^2, \bar{b}_i^1, \bar{b}_i^2, b_i^{1b}, b_i^{2b}, \bar{b}_i^{1b}, \bar{b}_i^{2b}, w_i, \bar{w}_i, w_i^b, \bar{w}_i^b \geq 0 \quad (68)$$

$$m_i, m_i^b, m_i^{gb} = \text{integer} \quad (69)$$

$$\delta_i, \bar{\delta}_i = \text{binary} \quad (70)$$

The stop time optimization is attached to the model BUS-AM-BAND in the same way as in the case of BUS-MULTIBAND, i.e., the model is supplemented with constraints Eq. (52), and s_i^b and $\bar{s}_i^b$ (sum of dwell time and additional waiting time) become decision-making variables. The optimization program BUS-AM-BAND S determines the decision variables b_i^1, $b_i^2 \bar{b}_i^1$, $\bar{b}_i^2$, b_i^{1b}, b_i^{2b}, $\bar{b}_i^1, \bar{b}_i^2, w_i, \bar{w}_i, w_i^b, \bar{w}_i^b, t_i, \bar{t}_i, t_i^b, \bar{t}_i^b, \delta_i, \bar{\delta}_i, m_i, m_i^b, m_i^{gb}, s_i^b$, and $\bar{s}_i^b$ with an objective function Eq. (53) and constraints Eqs. (54)–(70) and (52).

The presented models of the common coordination for general vehicles and public transport are much more complicated than MULTIBAND and AM-BAND. Table 1 compares the number of constraints and variables for MULTIBAND, BUS-MULTIBAND, and BUS-MULTIBAND S, and Table 2 compares AM-BAND, BUS-AM-BAND, and BUS-AM-BAND S. The number of variables increases almost 2 times for an artery with 10 intersections and 10 bus stops (90% for BUS-MULTIBAND and 88% for BUS-AM-BAND), and the number of constraints is more than 2 times greater. For models with stop time optimization, the number of variables and constraints is further increased by the variables and constraints associated with bus stops. Larger problem sizes with continuous variables do not cause computational difficulties currently, but the presented models contain 3 times more discrete variables than MULTIBAND and AM-BAND, resulting in much greater computational complexity.

Case Study

The effectiveness of the proposed methods was studied for an artery with dedicated bus lines in Cracow, Trzech Wieszczow Avenue, with 12 intersections. Data from this artery (Fig. 5) were used to evaluate the BUS-MULTIBAND and BUS-AM-BAND models and compare them with MULTIBAND and AM-BAND. The left side of the figure presents traffic data for general vehicles, in which, for readability, data only for the main street are presented. The numbers in parentheses represent traffic information for general vehicles; for example, (162, 148, 60) means that the total link volume is 370 vehicles/h, including 162 left-turn vehicles, 148 through vehicles, and 60 right-turn vehicles. For each intersection, the volume-to-capacity ratios for outbound and inbound traffic also are provided. The right side of the figure presents traffic data for public transport and bus stops' localization. The lines represent bus routes with the number of buses per hour. Distances between consecutive intersections and the ratios of inbound to outbound volumes of general vehicles for the corresponding sections also are provided. All intersections are controlled by a fixed-time strategy and have

Table 1. Constraints and variables for MULTIBAND, BUS-MULTIBAND, and BUS-MULTIBAND S

Type		MULTIBAND		BUS-MULTIBAND		BUS-MULTIBAND S	
Constraint	Variable	No. of constraints	No. of variables	No. of constraints	No. of variables	No. of constraints	No. of variables
Band	b_i, $\bar{b}_i$, b_i^b, $\bar{b}_i^b$	—	$2(n-1)$	—	$4(n-1)$	—	$4(n-1)$
Bandwidth	k_i, k_i^b	$(n-1)$	—	$2(n-1)$	—	$2(n-1)$	—
Cycle rate	z	2	1	2	1	2	1
Interference	w_i, $\bar{w}_i$, w_i^b, $\bar{w}_i^b$	$8(n-1)$	$2n$	$16(n-1)$	$4n$	$16(n-1)$	$4n$
Loop integer	m_i, m_i^b, m_i^{bg}	$(n-1)$	$(n-1)$	$3(n-1)$	$3(n-1)$	$3(n-1)$	$3(n-1)$
Travel time	t_i, $\bar{t}_i$, t_i^b, $\bar{t}_i^b$	$4(n-1)$	$2(n-1)$	$8(n-1)$	$4(n-1)$	$8(n-1)$	$4(n-1)$
Speed change	—	$4(n-2)$	—	$8(n-1)$	—	$8(n-1)$	—
Left-turn pattern	δ_i, $\bar{\delta}_i$	—	$2n$	—	$2n$	—	$2n$
Stop time	s_i^b, $\bar{s}_i^b$	—	—	—	—	n_b	$2n_b$
Total	—	$18n-20$	$9n-4$	$37n-35$	$17n-10$	$37n-35+n_b$	$17n-10+2n_b$
Example	$n=10$, $n_b=10$	160	84	345 (+116%)	160 (+90%)	355 (+122%)	180 (+114%)

Note: n_b = number of bus stops.

Table 2. Constraints and variables for AM-BAND, BUS-AM-BAND, and BUS-AM-BAND S

Type		AM-BAND		BUS-AM-BAND		BUS-AM-BAND S	
Constraint	Variable	No. of constraints	No. of variables	No. of constraints	No. of variables	No. of constraints	No. of variables
Band	b_i, $\bar{b}_i$, b_i^b, $\bar{b}_i^b$	—	$4(n-1)$	—	$8(n-1)$	—	$8(n-1)$
Bandwidth	k_i, k_i^b	$(n-1)$	—	$2(n-1)$	—	$2(n-1)$	—
Band asymmetry	—	$2(n-1)$	—	$4(n-1)$	—	$4(n-1)$	—
Cycle rate	z	2	1	2	1	2	1
Interference	w_i, $\bar{w}_i$, w_i^b, $\bar{w}_i^b$	$8(n-1)$	$2n$	$16(n-1)$	$4n$	$16(n-1)$	$4n$
Loop integer	m_i, m_i^b, m_i^{bg}	$(n-1)$	$(n-1)$	$3(n-1)$	$3(-1)$	$3(n-1)$	$3(n-1)$
Travel time	t_i, $\bar{t}_i$, t_i^b, $\bar{t}_i^b$	$4(n-1)$	$2(n-1)$	$8(n-1)$	$4(n-1)$	$8(n-1)$	$4(n-1)$
Speed change	—	$4(n-2)$	—	$8(n-1)$	—	$8(n-1)$	—
Left-turn pattern	δ_i, $\bar{\delta}_i$	—	$2n$	—	$2n$	—	$2n$
Stop time	s_i^b, $\bar{s}_i^b$	—	—	—	—	n_b	$2n_b$
Total	—	$20n-22$	$11n-6$	$41n-39$	$21n-14$	$41n-39+n_b$	$21n-14+2n_b$
Example	$n=10$, $n_b=10$	178	104	371 (+108%)	196 (+88%)	381 (+114%)	216 (108%)

J. Transp. Eng., Part A: Systems, 2020, 146(7): 04020051

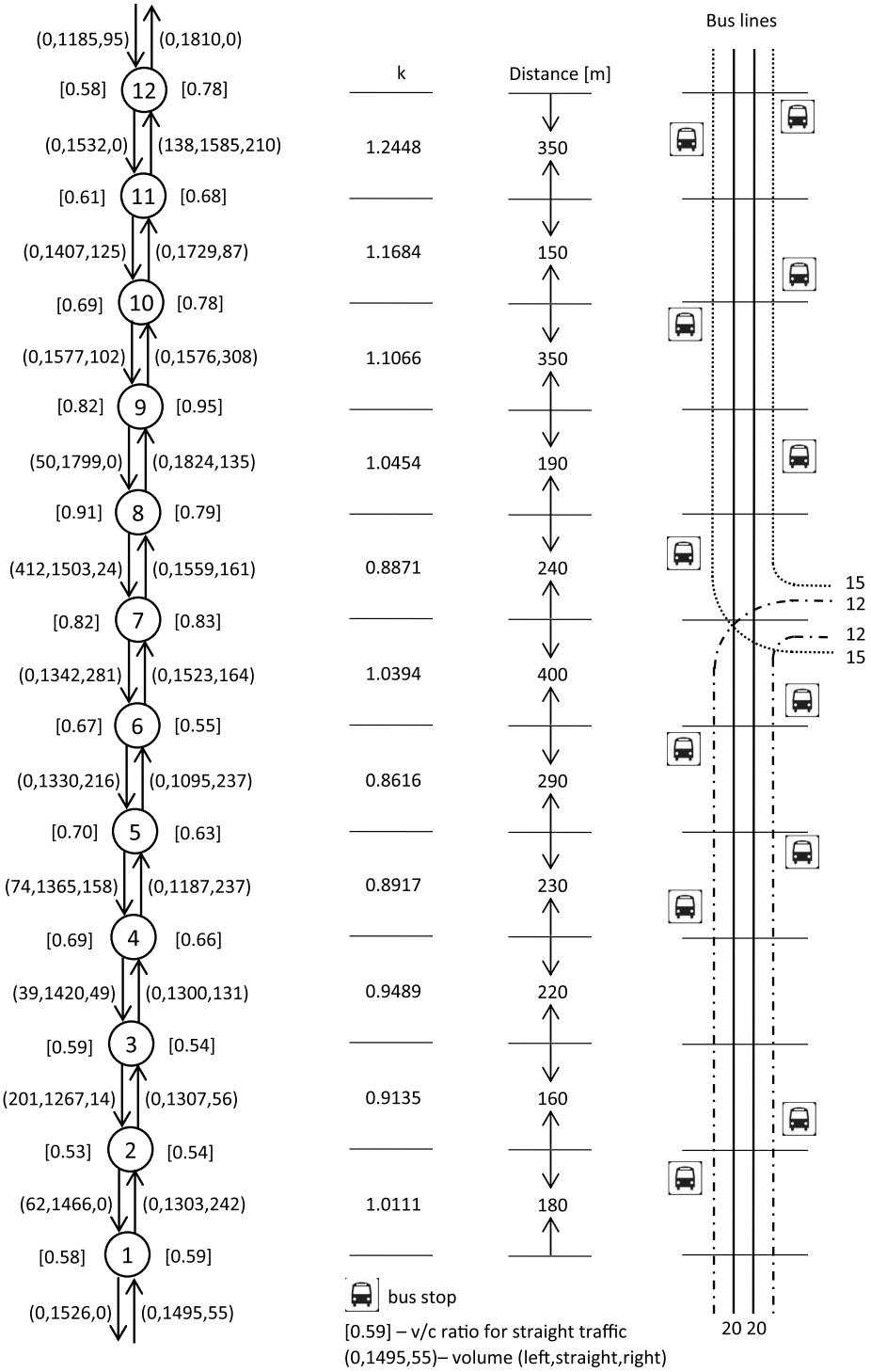

Fig. 5. Data for an arterial.

the same cycle length, which is one of the decision variables and may be optimized within established limits. For each version of the coordination problem, three scenarios were considered for different values of p, which is an exponential power that directly affects the weights for progression bandwidths. The presented models do not take into account the bus stop-time variability, but in the simulation model the stochasticity of dwell time is included as a variable with normal distribution with a mean value (20 s for basic models, and 20–40 s for models with stop-time optimization) and standard deviation of 5 and 10 s, respectively. A total of 36 scenarios were calculated in Octave, coded in Aimsun 8.2 and simulated for 50 replications. The mean and standard deviation of average delay and average number of stops for general vehicles and public transport were calculated.

Given input data such as red times, cycle time limits (Table 3), and distances between adjacent intersections, Octave was used to calculate the optimal signal coordination plans for the artery using the MULTIBAND, AM-BAND, BUS-MULTIBAND, and BUS-AM-BAND models and their variants with stop-time optimization. The signal control plans included bandwidth, travel time/speed,

Table 3. Control data for an arterial

	Intersection number											
	1	2	3	4	5	6	7	8	9	10	11	12
C	60–80 s											
r_i	0.208	0.250	0.250	0.383	0.408	0.375	0.425	0.383	0.400	0.367	0.208	0.367
$\overline{r_i}$	0.125	0.250	0.250	0.383	0.408	0.375	0.300	0.383	0.400	0.367	0.208	0.283
L_i	0	0	0	0	0	0	0	0	0	0	0	0.133
$\overline{L_i}$	0.083	0	0	0	0	0	0.167	0	0	0	0	0

interference values for general vehicles and public transport, and common parameters such as cycle length and left-turn pattern. The optimized traffic signal control plans were evaluated using the Aimsun simulation model. A desktop computer was used in this study with an AMD Phenom II X4 965 CPU, 8 GB RAM, and 64-bit Windows 7 operating system. For this problem, whereas the calculation times for MULTIBAND and AM-BAND did not exceed a few seconds, calculation times for BUS-MULTIBAND and BUS-AM-BAND were much longer, and in the worst case the calculation time exceeded 3 minutes. However, in most cases Octave was able to find the optimal solution in about 1 min.

Time-Space Diagrams

The selected traffic signal coordination plans generated by Octave for MULTIBAND, BUS-MULTIBAND, and BUS-MULTIBAND S are presented in the form of time–space diagrams in Fig. 6. The time-space diagrams for AM-BAND, BUS-AM-BAND, and BUS-AM-BAND S are presented in Fig. 7. The bus progression bands usually are wide; therefore, it is expected that the variability of the stopping time will not significantly decrease the efficiency for buses.

Aimsun Simulation Results

The simulation results, i.e., the average delay time and the average number of stops for the MULTIBAND and both versions of the BUS-MULTIBAND methods, are presented in Table 4. Similar results for the AM-BAND and both versions of the BUS-AM-BAND methods are presented in Table 5. Measures of effectiveness (MOEs) were calculated for two classes of vehicles: general vehicles, and public transport vehicles. For the latter, MOEs were calculated for two values of stop-time standard deviation (5 and 10 s). The average delay was calculated as the average of the delay time of each vehicle per kilometer, and had units of seconds per vehicle per kilometer. The average number of stops was calculated as the average of the number of stops of each vehicle per kilometer, and had units of number of stops per vehicle per kilometer, but for the buses this did not include stops at bus stops (i.e., it included stops caused by traffic lights only). For both measures of effectiveness, the mean value and standard deviation (in parentheses) was presented. The standard deviations were small enough compared with the means, which suggests that the results are statistically significant.

The MULTIBAND and AM-BAND methods gave very similar results for both classes of vehicles, but both MOEs for public transport improved with the increase in bus stop-time variability, which means that shorter or longer than average stopping time allows some buses to use progression bands intended for cars. BUS-MULTIBAND and BUS-AM-BAND provided significant improvements in terms of all MOEs for buses, with usually small changes for general vehicles for $p = 0$, but for $p = 1$ BUS-AM-BAND clearly outperformed BUS-MULTIBAND. For $p = 2$ with such weighting coefficients, passenger cars, for which the volume-to-saturation flow rate ratio usually is higher, were strongly favored, bus progression bands were narrow, and the effectiveness of both methods for transit vehicles was rather low. Models with stop-time optimization, i.e., BUS-MULTIBAND S and BUS-AM-BAND S, clearly reduced the average delay time and number of stops, with usually minor changes for general vehicles for $p = 0$ and 1, but for $p = 2$, only BUS-MULTIBAND S gave significant improvements in both MOEs. Comparing MOEs for buses for different standard deviations in stop time indicates that the solutions generated by the proposed methods are moderately sensitive to stop-time variability.

To better illustrate the relative improvements brought by proposed methods compared with MULTIBAND and AM-BAND, the percentage changes in terms of the average delay and the average number of stops were calculated. Table 6 compares BUS-MULTIBAND and BUS-MULTIBAND S to MULTIBAND in terms of all MOEs.

BUS-MULTIBAND can reduce delay up to 6.7% for low stop-time variability and up to 5.1% for high stop-time variability for buses at the expense of an increase of 5.9% for cars ($p = 0$). BUS-MULTIBAND S gives much better results; it can reduce delays by up to 22.2% (std 5) or 18.3% (std 10) for buses and 3.9% for cars ($p = 1$). BUS-MULTIBAND can reduce the average number of stops by up to 15.3% (std 5) or 9.6% (std 10) for buses and 3.7% for cars ($p = 0$). BUS-MULTIBAND S can reduce the number of stops by up to 42.6% (std 5) or 34.8% (std 10) for buses and 14.3% for cars ($p = 1$).

Table 7 compares BUS-AM-BAND and BUS-AM-BAND S with AM-BAND in terms of all MOEs. BUS-AM-BAND can reduce delay by up to 9.7% (std 5) or 6.3% (std 10) for buses at the expense of an increase of 6.3% for cars ($p = 0$). BUS-AM-BAND S can reduce delay by up to 16.8% (std 5) or 14.4% (std 10) for buses at the expense of a negligible increase of 0.3% for cars ($p = 0$). BUS-AM-BAND can reduce the average number of stops by up to 28.1% (std 5) or 24.9% (std 10) for buses at the expense of a significant increase of 20.4% for cars ($p = 0$). BUS-AM-BAND S improved the average number of stops by up to 33% (std 5) or 29.6% (std 10) for buses and 4.4% for cars ($p = 0$).

Usually, the improvement of MOE for buses is at the expense of deterioration of MOE for cars; however, the benefit for buses usually is much higher than the loss for cars. In some cases there are improvements of MOE for both classes of vehicles, which is because some cars use a bandwidth prepared for buses. The proposed models do not take into account the bus stop-time variability, but the simulation results simulations indicate that even at considerable dwell-time variability, the methods provide significant improvements in terms of bus average delay and number of stops. The study was conducted for a relatively short cycle time (60–66 s depending on the case). It can be expected, however, that for longer cycle times or shorter green times for coordinated direction, the importance of additional progression bands prepared for buses will increase.

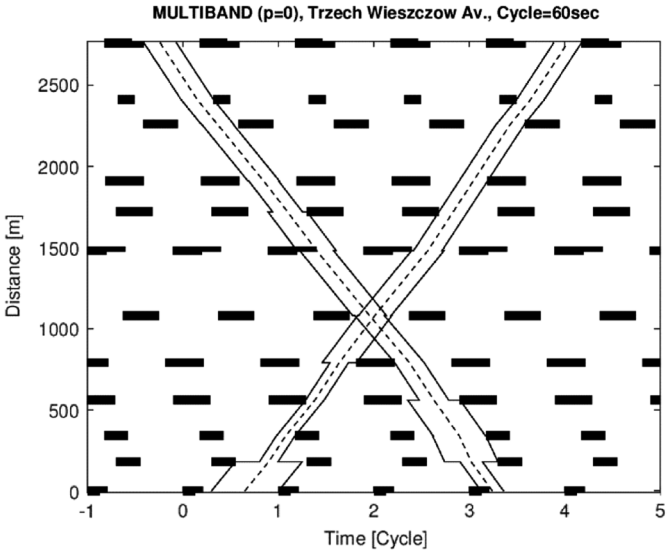

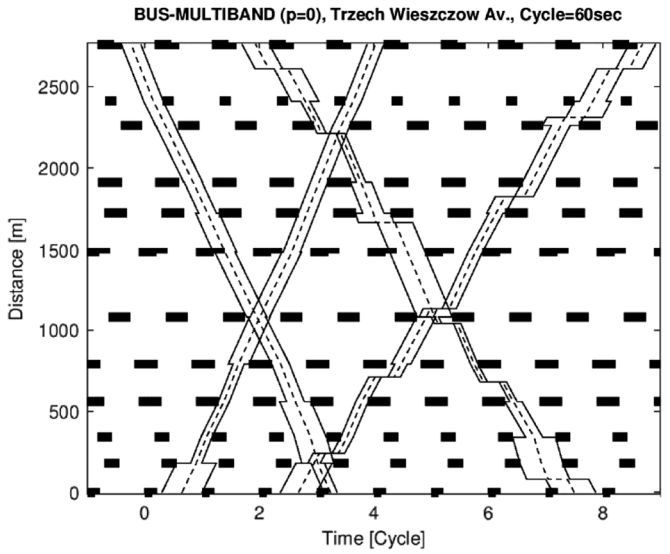

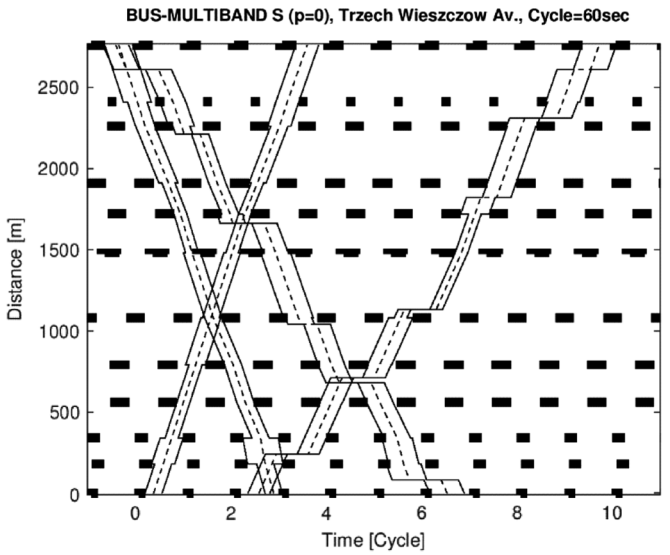

Fig. 6. MULTIBAND, BUS-MULTIBAND, and BUS-MULTIBAND S time-space diagrams.

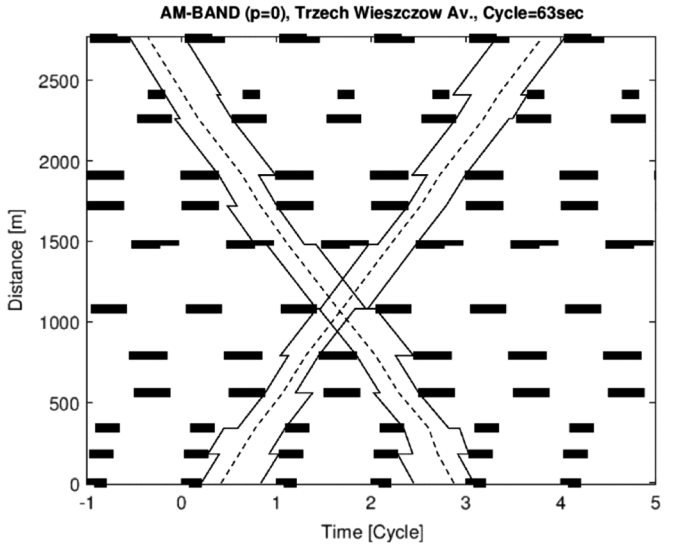

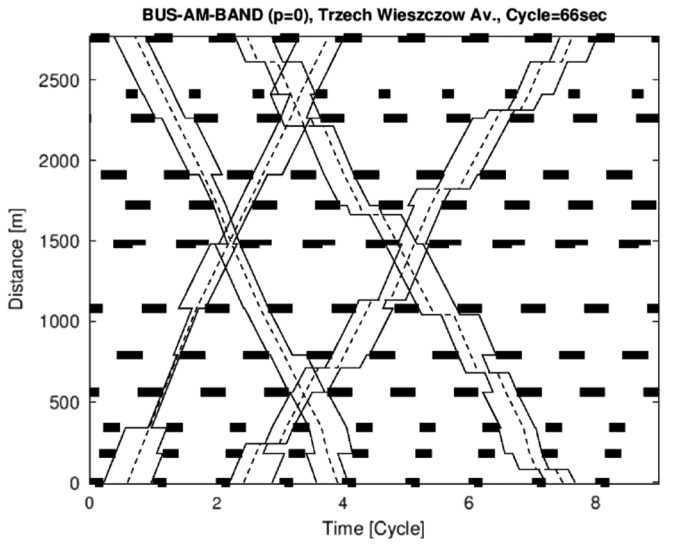

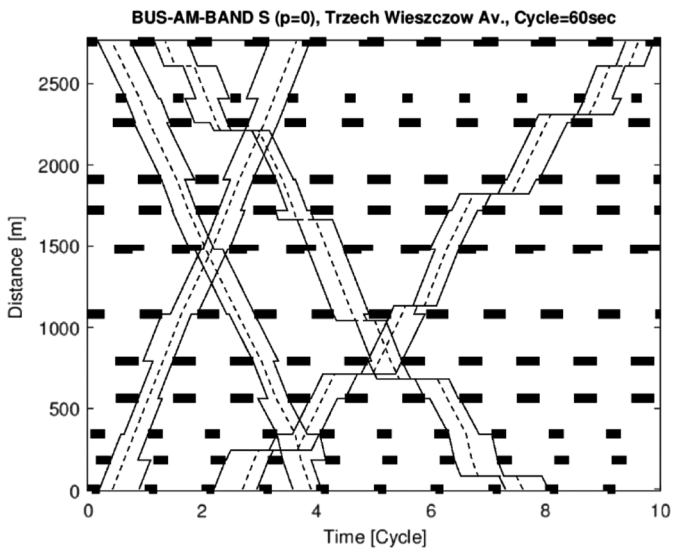

Fig. 7. AM-BAND, BUS-AM-BAND, and BUS-AM-BAND S, time-space diagrams.

Table 4. Simulation results for MULTIBAND, BUS-MULTIBAND, and BUS-MULTIBAND S

		Average delay (s/vehicle/km)						Number of stops (no./vehicle/km)					
Method	p	Car		Bus (std 5)		Bus (std 10)		Car		Bus (std 5)		Bus (std 10)	
MULTIBAND	0	78.17	(2.02)	49.35	(1.08)	46.96	(1.57)	1.37	(0.02)	1.37	(0.06)	1.24	(0.03)
	1	79.88	(1.90)	51.31	(1.28)	49.25	(1.66)	1.46	(0.02)	1.37	(0.04)	1.30	(0.10)
	2	80.09	(1.85)	50.31	(1.00)	47.89	(1.59)	1.49	(0.01)	1.34	(0.04)	1.27	(0.05)
BUS-MULTIBAND	0	82.76	(2.69)	46.06	(1.50)	44.57	(1.58)	1.32	(0.01)	1.16	(0.08)	1.12	(0.04)
	1	83.61	(2.78)	49.91	(1.35)	48.03	(1.68)	1.40	(0.02)	1.36	(0.08)	1.29	(0.05)
	2	79.89	(1.90)	50.81	(1.32)	48.76	(1.60)	1.45	(0.01)	1.39	(0.07)	1.26	(0.08)
BUS-MULTIBAND S	0	81.85	(2.81)	40.65	(1.53)	40.29	(1.65)	1.48	(0.02)	0.88	(0.07)	0.86	(0.08)
	1	76.78	(2.11)	39.92	(1.52)	40.25	(1.46)	1.25	(0.02)	0.79	(0.06)	0.85	(0.07)
	2	78.34	(1.98)	43.75	(1.52)	43.68	(1.69)	1.33	(0.01)	1.06	(0.06)	1.05	(0.04)

Table 5. Simulation results for AM-BAND, BUS-AM-BAND, and BUS-AM-BAND S

		Average delay (s/vehicle/km)						Number of stops (no./vehicle/km)					
Method	p	Car		Bus (std 5)		Bus (std 10)		Car		Bus (std 5)		Bus (std 10)	
AM-BAND	0	78.13	(2.06)	49.09	(1.37)	47.31	(1.44)	1.32	(0.03)	1.38	(0.07)	1.28	(0.06)
	1	78.25	(2.03)	49.35	(1.43)	46.88	(1.34)	1.35	(0.02)	1.35	(0.05)	1.26	(0.04)
	2	78.55	(2.08)	48.1	(1.32)	46.67	(1.42)	1.34	(0.02)	1.31	(0.03)	1.25	(0.03)
BUS-AM-BAND	0	83.07	(1.87)	44.34	(1.18)	44.32	(1.55)	1.59	(0.01)	0.99	(0.04)	0.96	(0.04)
	1	80.97	(2.76)	47.58	(1.54)	45.8	(1.48)	1.28	(0.01)	1.19	(0.04)	1.16	(0.06)
	2	77.67	(2.02)	47.91	(1.71)	47.24	(1.50)	1.28	(0.02)	1.31	(0.04)	1.26	(0.03)
BUS-AM-BAND S	0	78.37	(2.05)	40.83	(1.32)	40.52	(1.40)	1.26	(0.02)	0.93	(0.05)	0.90	(0.04)
	1	81.16	(2.70)	41.07	(1.18)	40.64	(1.68)	1.29	(0.02)	0.93	(0.04)	0.92	(0.04)
	2	78.24	(2.02)	47.03	(1.38)	45.67	(1.38)	1.35	(0.03)	1.27	(0.06)	1.19	(0.07)

Table 6. Comparison of BUS-MULTIBAND and BUS-MULTIBAND S with MULTIBAND

		Change compared with MULTIBAND (%)					
		Average delay			Number of stops		
Method	p	Car	Bus (std 5)	Bus (std 10)	Car	Bus (std 5)	Bus (std 10)
BUS-MULTIBAND	0	5.9	−6.7	−5.1	−3.7	−15.3	−9.6
	1	4.7	−2.7	−2.5	−4.1	−1.2	−0.8
	2	−0.2	1.0	1.8	−2.4	3.5	−0.8
BUS-MULTIBAND S	0	4.7	−17.6	−14.2	8.2	−35.3	−30.3
	1	−3.9	−22.2	−18.3	−14.3	−42.6	−34.8
	2	−2.2	−13.0	−8.8	−10.7	−20.9	−17.3

Table 7. Comparison of BUS-AM-BAND and BUS-AM-BAND S to AM-BAND

		Change compared with AM-BAND (%)					
		Average delay			Number of stops		
Method	p	Car	Bus (std 5)	Bus (std 10)	Car	Bus (std 5)	Bus (std 10)
BUS-AM-BAND	0	6.3	−9.7	−6.3	20.4	−28.1	−24.9
	1	3.5	−3.6	−2.3	−5.0	−11.9	−7.9
	2	−1.1	−0.4	1.2	−5.0	0.2	1.0
BUS-AM-BAND S	0	0.3	−16.8	−14.4	−4.4	−33.0	−29.6
	1	3.7	−16.8	−13.3	−4.1	−31.5	−27.0
	2	−0.4	−2.2	−2.1	0.4	−2.5	−4.6

The proposed approach suffers from some limitations. It does not take into account the dwell-time variability, and additional studies should focus on this problem. Moreover, the choice of weighting coefficients in the objective function needs further research.

Conclusions

This study investigated the problem of simultaneous coordination for general and public transport vehicles. The proposed BUS-MULTIBAND and BUS-AM-BAND methods are based on the

wellknown MULTIBAND and AM-BAND models, respectively. The common coordination models for general and public transport vehicles were formed by incorporating additional bands for buses into basic MULTIBAND and AM-BAND methods. The BUS-MULTIBAND and BUS-AM-BAND models and their variations with stop-time optimization (BUS-MULTIBAND S and BUS-AM-BAND S) were formulated as mixed-integer linear programs and solved by Octave. Their performance including bus stop-time variability was compared with that of MULTIBAND and AM-BAND based on a case study artery using Aimsun simulations.

The optimal solutions were evaluated in terms of average delay and number of stops. The simulation results consistently showed that the overall performance of BUS-MULTIBAND and BUS-AM-BAND was better for public transport vehicles than those of MULTIBAND and AM-BAND at the expense of at most a small deterioration for general vehicles. The greatest benefits for public transport, and often for general vehicles as well, were from models with stop-time optimization (BUS-MULTIBAND S and BUS-AM-BAND S).

Different weighting strategies (i.e. p-value) also were considered. For BUS-MULTIBAND and BUS-AM-BAND and their variations, the results varied for different p-values. For models without stop-time optimization (BUS-MULTIBAND, BUS-AM-BAND), efficiency decreased with increasing p-value. For larger values of p, the proposed methods gave a slight improvement for buses, because the weighting coefficients, i.e., the volume-to-saturation flow ratio in the objective function, always were less than 1 and usually were smaller for buses than for general vehicles. A large exponential power p strongly reduces low weighting coefficients of the objective, and hence the bandwidths for buses are much narrower than for other vehicles. For models with stop-time optimization (BUS-MULTIBAND S, BUS-AM-BAND S) all considered values of p were suitable, but there was a clear relationship between the value of p and the improvement of MOEs: the greatest benefits were for small p-values.

The proposed methods can improve the quality of public transport services by reducing the average delay and number of stops caused by traffic signals and can improve schedule reliability without significant losses for general traffic. These methods can be considered as a passive priority strategy and can be supplemented with active priority (green extension or early start). After a passive priority solution is obtained, active priority can be applied, which can further improve the efficiency of public transport vehicles and ensure smooth intersection passage without stopping.

Notation

The following symbols are used in this paper:

$b_i(\bar{b}_i)$ = outbound (inbound) bandwidth for segment i (cycles);
$b_i^b(\bar{b}_i^b)$ = bus outbound (inbound) bandwidth for segment i (cycles);
$C_{\min}$, $C_{\max}$ = lower and upper limits of cycle length (s);
$d_{i,i+1}(\bar{d}_{i,i+1})$ = distance between intersections S_i and S_{i+1} outbound (inbound) (m);
e_i, $f_i(\bar{e}_i, \bar{f}_i)$ = lower/upper limits of outbound (inbound) speed (m/s);
e_i^b, $f_i^b(\bar{e}_i^b, \bar{f}_i^b)$ = lower/upper limits of outbound (inbound) bus speed (m/s);
g_i, $h_i(\bar{g}_i, \bar{h}_i)$ = lower/upper limits of change in outbound (inbound) speed (m/s);
g_i^b, $h_i^b(\bar{g}_i^b, \bar{h}_i^b)$ = lower/upper limits of change in outbound (inbound) bus speed (m/s);
k_i = target ratios of inbound to outbound bandwidth on section i;
k_i^b = bus target ratios of inbound to outbound bandwidth on section i;
$L_i(\bar{L}_i)$ = time allocated for outbound (inbound) left-turn green at S_i (cycles);
m_i = loop integer variable;
m_i^b = bus loop integer variable;
m_i^{bg} = public/general vehicle integer variable;
$p = 0$, 1, and 2 = exponential power;
$r_i(\bar{r}_i)$ = outbound (inbound) red time at intersection S_i (cycles);
$S_i^b(\bar{S}_i^b)$ = outbound (inbound) bus saturation flow on section i;
$s_i^b(\bar{s}_i^b)$ = stop time of bus stop i outbound (inbound);
s_i^{bd} = dwell time of bus stop i (uncontrollable) (cycles);
s_i^{bw} = waiting time at bus stop i (controllable) (cycles);
$s_{i\min}^b$ ($\bar{s}_{i\min}^b$) = minimum stop time at bus stop i outbound (inbound) (cycles);
$s_{i\max}^b$ ($\bar{s}_{i\max}^b$) = maximum stop time at bus stop i outbound (inbound) (cycles);
std = standard deviation of bus stop time (s);
$t_{i,i+1}(\bar{t}_{i,i+1})$ = travel time from S_i to S_{i+1} outbound (S_{i+1} to S_i inbound) (cycles);
$t_{i,i+1}^b(\bar{t}_{i,i+1}^b)$ = bus travel time from S_i to S_{i+1} outbound (S_{i+1} to S_i inbound) (cycles);
$V_i^b(\bar{V}_i^b)$ = outbound (inbound) total directional bus volume on section i;
$w_i(\bar{w}_i)$ = interference variables (cycles);
$w_i^b(\bar{w}_i^b)$ = bus interference variables (cycles);
$z = 1/C$ = signal frequency (cycles/s);
Δ_i = intranode offset, i.e., time difference between center of r_i and nearest center of $\bar{r}_i$; Δ_i is positive if center of r_i is to right of center of $\bar{r}_i$ (cycles);
$\tau_i(\bar{\tau}_i)$ = outbound (inbound) queue clearance time at S_i (cycles);
$\tau_i^b(\bar{\tau}_i^b)$ = outbound (inbound) bus queue clearance time at S_i (cycles);
δ_i, $\bar{\delta}_i$ = binary variables through which left-turn pattern is determined;
$\Phi_{i,i+1}$ ($\bar{\Phi}_{i,i+1}$) = internode offsets (cycles); and
$\Phi_{i,i+1}^b$ ($\bar{\Phi}_{i,i+1}^b$) = bus internode offsets (cycles).

References

Chang, E. C. P., S. L. Cohen, C. Liu, N. A. Chaudhary, and C. Messer. 1988. "MAXBAND-86: Program for optimizing left-turn phase sequence in multi-arterial closed networks." *Transp. Res. Rec.* 1181 (1): 61–67.

Chaudhary, N. A., and C. J. Messer. 1993. "PASSER-IV: A program for optimizing signal timing in grid networks." *Transp. Res. Rec.* 1421 (1): 82–93.

Dai, G. Y., H. Wang, and W. Wang. 2016. "Signal optimization and coordination for bus progression based on MAXBAND." *KSCE J. Civ. Eng.* 20 (2): 890–898. https://doi.org/10.1007/s12205-015-1516-4.

Gartner, N. H., S. F. Assmann, F. L. Lasaga, and D. L. Hou. 1991. "A multi-band approach to arterial traffic signal optimization." *Transp. Res. B* 25 (1): 55–74. https://doi.org/10.1016/0191-2615(91)90013-9.

Gartner, N. H., and C. Stamatiadis. 2002. "Arterial-based control of traffic flow in urban grid networks." *Math. Comput. Modell.* 35 (5–6): 657–671. https://doi.org/10.1016/S0895-7177(02)80027-9.

Jeong, Y., and Y. Kim. 2014. "Tram passive signal priority strategy based on the MAXBAND model." *KSCE J. Civ. Eng.* 18 (5): 1518–1527. https://doi.org/10.1007/s12205-014-0159-1.

Kim, H., Y. Cheng, and G.-L. Chang. 2019. "Variable signal progression bands for transit vehicles under dwell time uncertainty and traffic queues." *IEEE Trans. Intell. Transp. Syst.* 20 (1): 109–122. https://doi.org/10.1109/TITS.2018.2801567.

Little, J. D. 1966. "The synchronization of traffic signals by mixed-integer linear programming." *Oper. Res.* 14 (4): 568–594. https://doi.org/10.1287/opre.14.4.568.

Little, J. D. C., M. D. Kelson, and N. H. Gartner. 1981. "MAXBAND: A program for setting signals on arterials and triangular networks." *Transp. Res. Rec.* 759 (1): 40–46.

Lu, S., X. Liu, and S. Dai. 2008. "Revised MAXBAND model for bandwidth optimization of traffic flow dispersion." In *Proc., 2008 ISECS Int. Colloquium on Computing, Communication, Control, and Management*, 85–89. Piscataway, NJ: IEEE. https://doi.org/10.1109/CCCM.2008.251.

Ma, W., L. Zou, K. An, N. H. Gartner, and M. Wang. 2019. "A partition-enabled multi-mode band approach to arterial traffic signal optimization." *IEEE Trans. Intell. Transp. Syst.* 20 (1): 313–322. https://doi.org/10.1109/TITS.2018.2815520.

Morgan, J. T., and J. D. Little. 1964. "Synchronizing traffic signals for maximal bandwidth." *Oper. Res.* 12 (6): 896–912. https://doi.org/10.1287/opre.12.6.896.

Pillai, R. S., A. K. Rathi, and S. L. Cohen. 1998. "A restricted branch-and-bound approach for generating maximum bandwidth signal timing plans for traffic networks." *Transp. Res. B* 32 (8): 517–529. https://doi.org/10.1016/S0191-2615(96)00033-1.

Stamatiadis, C., and N. H. Gartner. 1996. "MULTIBAND-96: A program for variable-bandwidth progression optimization of multiarterial traffic networks." *Transp. Res. Rec.* 1554 (1): 9–17. https://doi.org/10.1177/0361198196155400102.

Tian, Z., V. Mangal, and H. Liu. 2008. "Effectiveness of lead-lag phasing on progression bandwidth." *Transp. Res. Rec.* 2080 (1): 22–27. https://doi.org/10.3141/2080-03.

Tian, Z., and T. Urbanik. 2007. "System partition technique to improve signal coordination and traffic progression." *J. Transp. Eng.* 133 (2): 119–128. https://doi.org/10.1061/(ASCE)0733-947X(2007)133:2(119).

Yang, X., Y. Cheng, and G.-L. Chang. 2015. "A multi-path progression model for synchronization of arterial traffic signals." *Transp. Res. C* 53 (1): 93–111. https://doi.org/10.1016/j.trc.2015.02.010.

Zhang, C., Y. Xie, N. H. Gartner, C. Stamatiadis, and T. Arsava. 2015. "AM-Band: An asymmetrical multi-band model for arterial traffic signal coordination." *Transp. Res. C* 58 (1): 515–531. https://doi.org/10.1016/j.trc.2015.04.014.

Zhang, L., Z. Song, X. Tang, and D. Wang. 2016. "Signal coordination models for long arterials and grid networks." *Transp. Res. C* 71 (1): 215–230. https://doi.org/10.1016/j.trc.2016.07.015.

Zhou, H., H. G. Hawkins, and Y. Zhang. 2017. "Arterial signal coordination with uneven double cycling." *Transp. Res. A* 103 (1): 409–429. https://doi.org/10.1016/j.tra.2017.07.004.

Zhou, Y., S. Jia, B. Mao, T. K. Ho, and W. Wei. 2016. "An arterial signal coordination model for trams based on modified AM-BAND." In *Discrete dynamics in nature and society.* London and New York: Hindawi. https://doi.org/10.1155/2016/5028095.